Afghanistan Journal of Infectious Diseases
AJID
https://ajid.ghalib.edu.af/index.php/ajid
Vol. 2, No.2, July 2024, pp. 57-76

Analyzing the Dynamic Characteristics of a Tuberculosis Epidemic Model Using Numerical Methods

Zabihullah Movaheedi[1*]

1. Department of Mathematics, Faculty of Science, University of Herat, Herat, Afghanistan.

ARTICLE INFO

Type: Original Article
Recevied: 2024/1/9
Accepted: 2024/6/11

***Corresponding Author:**
Zabihullah Movaheedi
Address: Department of Mathematics, Faculty of Science, University of Herat, Herat -3001, Afghanistan.

z.movaheedi@hu.edu.af

ABSTRACT

Introduction: This study aims to assess the performance of an analytical model for tuberculosis transmission using different numerical approaches and to compare the effectiveness of these methods in simulating disease behavior under various conditions.

Methods: This paper analyzes the dynamics of tuberculosis using the VSEIT epidemiological model and the numerical method NSFD (Non-Standard Finite Difference). The VSEIT model describes the community in terms of five key populations: vaccinated (V), susceptible (S), exposed (E), infected (I), and treated (T). The results demonstrate that the NSFD method is effective in accurately capturing the dynamic characteristics of the proposed model and also confirms the local and global stability of the disease equilibrium.

Results: Simulation results demonstrate that the NSFD method is a unique and effective approach for controlling and predicting the spread of tuberculosis. This comparison underscores the effectiveness of this method compared to traditional Euler and fourth-order Runge-Kutta (RK4) methods.

Conclusion: The importance and effectiveness of the NSFD method in modeling the dynamic nature of tuberculosis are highlighted. This study is a valuable recommendation for policymakers and public health officials by providing concrete insights into the control and prediction of tuberculosis spread, thereby enhancing the efficacy of intervention strategies.

Kewwors: Tuberculosis, Epidemic modeling, Numerical methods, Non-standard finite difference (NSFD) and Reproductive model.

To cite this article: Movaheedi Z. Analyzing the Dynamic Characteristics of a Tuberculosis Epidemic Model Using Numerical Methods. Afghanistan Journal of Basic Medical Sciences . 2024 July;2 (2):57-76. https://doi.org/10.60141/AJID/V.2.I.2/8

1. Introduction

Mycobacterium tuberculosis, a bacterium, is the source of the infectious illness known as TB. It mostly has an impact on the lungs. Additionally, it can spread to different body areas, such as the spine and brain. It is important to note that indirect touch is another way to contract it. Both with an infected person as well as by breathing in airborne droplets carrying the microbes. When TB patients cough, polluted air is discharged into the air and disseminated by the germs that cause TB. TB is the second-leading cause of death among illnesses brought on by a single infectious agent. The sickness that is fatal everywhere, One of the top 10 killers in the world, TB affects 1.8 million lives globally. In 2020, 86% of all new TB cases were found in the 30 nations with the greatest burden of illness. According to the World Health Organization (WHO), Eight countries, with India leading the pack, are responsible for two-thirds of the cases, with China, Indonesia, the Philippines, Pakistan, Nigeria, Bangladesh, and South Africa following (1). This indicates how the spread of TB endangers human health and impacts social and economic life (2-4).

Mathematical modeling allows researchers to simulate the spread of infectious diseases, taking into account various factors such as population size, transmission rates, and intervention measures (5-7). By analyzing these models, policymakers can make informed decisions on implementing control strategies and interventions to mitigate the impact of the epidemic (8). Additionally, mathematical modeling also helps in predicting future outbreaks and identifying areas that require immediate attention and resources. The study of mathematical modeling of infectious illnesses has gained popularity during the 20th century. The older works in this area are available in. To control TB efforts involves the use of mathematical models extensively. Understanding an epidemic's dynamics with the use of modeling can help contain its spread. Additionally, models help with disease control and epidemic forecasting (9, 10). Bernoulli made the first work on the mathematical modeling of illness transmission in 1766 (11). P.D. En'ko is recognized for making several significant contributions to mathematical epidemiology between 1873 and 1894. However, it might be stated that Sir Ronald Ross presented the first mathematical model of malaria transmission in 1911.

This laid the foundation for mathematical epidemiology based on compartmental models. Compartmental models clearly take into account the many stages of illness progression and the transitions between them, which distinguishes them from other disease models. This enables a more thorough comprehension of the spread of illnesses and the implementation of actions to stop that spread (11). Their findings suggest that there is a decrease in the prevalence of the virus and a reduction in the significance of the smart crown infection [12–15]. During COVID-19 vaccination, the virus's spike proteins attach to ACE2 receptors, allowing the RNA to enter our cells and create more COVID-19 viruses. This process spreads the infection to other cells (16).

The study of epidemiology is important in various fields such as engineering, chemistry, medicine, economics, and physics (17). Various mathematical models have been examined, as detailed in (18). These models illustrate situations in which variability occurs. Although numerical schemes converge, it is unclear if they preserve the system's dynamic properties (19). To achieve symmetry with the continuous model and solve such problems, a

stochastic nonstandard finite difference method must be constructed (20). There are four compartments in the delayed epidemic model of diarrhea: susceptible, infective, treated, and recovered. The model has a saturated incidence rate structured in the artificial delay parameter (21).

The dynamics of tuberculosis morbidity are determined by mathematical models of epidemiological processes that are taken into consideration in the survey. In the early 1960s of this century, the first models of tuberculosis epidemiology were created and released (22). Epidemiologists who love mathematics pioneered the study of epidemic transmission (23–25). The follow-up will demonstrate that, despite these limitations, the fatigue of susceptible individuals in the community does not always indicate the end of an epidemic (26). Mathematical modeling is a crucial tool for understanding the spread of diseases and developing effective control strategies. Over the past few decades, a number of biologists and mathematicians have developed various epidemic models to study the dynamics of tuberculosis in different parts of the world (27). Since it was initially believed to have a negative effect on those already infected with . tuberculosis, the vaccine was limited to tuberculin-negative children, as it was not expected to be beneficial for them (28).

The susceptible-exposed- Infected - Recovered (SEIR) model, which incorporates the exposed group, significantly enhances the SIR model (29). The SEIR model was first used by Aron and Schwartz (31) to examine the significance of seasonality in epidemic transmission. Li et al.'s (30) analysis of the SEIR model's global dynamics with a changing population size. An SEIR model was created by Newton and Reiter (26) to study dengue fever's behavior. SEIR models were then utilized in the research on TB. Compartmental models used in epidemiology may be generally divided into two groups: models employing differential equations to describe the dynamics of infectious illness functions that are continuous and may record the ongoing changes in state variables across Systems of ordinary differential equations and difference equations are commonly used to depict time. Models of equations are frequently employed when facts are accumulated at discrete time intervals or when a discrete technique is superior at capturing population dynamics (33).

The relevance of vaccination for TB mathematical modeling depends on making forecasts about curing the illness. Numerous earlier investigations are included. With regard to this subject, the objective of (9) was to ascertain the dynamics of TB. A mathematical formula was created by Egonmwan et al. in a framework that includes vaccination of infants and elderly vulnerable individuals in the dynamics of TB transmission in a community in an effort to safeguard people of all ages who are vulnerable (10). Models for the distribution of economic resources were developed by Revelle et al. (11). Some measures were used to combat TB.

To better understand the dynamics of the TB infection, we suggest a VSEIT epidemiological model in this work. We computed the parameters of the biological model to validate its performance. nursing particular TB data, such as illness prevalence, incidence, and other pertinent data on epidemiology from 1990 to 2020 taken from the WHO Global TB Report (1). The author of the research paper used different methodologies, such as Euler, RK-4, and a discrete NSFD system. The NSFD method was specifically designed to investigate aspects related to biological sustainability and other model characteristics. The goal was to use strategies like Euler, RK-4, and the advanced

NSFD to control the spread of TB and assess potential public health risks. Notably, the NSFD approach was effective across various step sizes, producing positive outcomes. Additionally, the study examined the local and global stability of disease-free equilibria within the NSFD framework. These equilibria were found to be suitable and unconditionally stable for the continuous model, and a comparison revealed their precision and efficacy.

This paper is structured as follows: In Section 2, we introduce the TB scourge model and make sense of its related boundaries. Section 3 outlines the current equilibrium and reproduction numbers for the deterministic model. Section 4 discusses the local and global stability of disease-free for the continuous model, utilizing the generation number. In Section 5, we develop the Euler, RK-4, and discrete NSFD schemes to examine the convergence and divergence of disease-free states for the proposed model. Our computations demonstrate that the NSFD scheme is an effective and robust method, providing a clear representation of the continuous model. Mathematical simulations are also included to reinforce our theoretical results. Finally, the last section presents a brief conclusion.

2. Various basic mechanisms characteristically type of a mathematical model

In this paper, we analyze the dynamics of tuberculosis (TB) disease using a VSEIT epidemiological model. To classify the entire population, five classes are used, i.e., vaccinated persons, susceptible persons, exposed persons, infected persons, and treated persons.

$$\begin{aligned}
\frac{\mathrm{dV}}{\mathrm{dt}} &= qv - (m+\eta)V(t)\\
\frac{\mathrm{dS}}{\mathrm{dt}} &= (1-q)v + mV(t) - \beta S(t)I(t) - \eta S(t)\\
\frac{\mathrm{dE}}{\mathrm{dt}} &= \beta S(t)I(t) - (\psi+\eta)E(t) + (1-\gamma)dT(t)\\
\frac{\mathrm{dI}}{\mathrm{dt}} &= \psi E(t) + \gamma dT(t) - (\theta+\eta+\nabla)\mathrm{I(t)}\\
\frac{\mathrm{dT}}{\mathrm{dt}} &= \theta I(t) - (\eta+d+\phi)T(t).
\end{aligned} \tag{1}$$

Here $V(t) \geq 0, S(t) \geq 0, E(t) \geq 0, I(t) \geq 0,$ and $T(t) \geq 0$ with $N \geq 0$.

Figure 1. shows the model flowchart and Table 1. lists the variables and parameters.

3. Equilibrium and reproduction number $(\boldsymbol{R_0})$

3.1. Equilibria of model

The TB-free (TFE) point is get by putting the equations (1) of given model is equal to zero. The system give us, $E_0 = (V^0, S^0, E^0, I^0, T^0)$ for model (1), then it is easy to search out the TFE $E_0 = \left(\frac{qv}{(m+\eta)}, \frac{(1-q)v}{\eta}, 0,0,0\right)$.

The given model (1) is all together the state variables were resolved $V, S, E, I,$ and T to find the TB endemic equilibrium (TEE) point.

If the TEE point is represented by $E^*(V^*, S^*, E^*, I^*, T^*)$, then model (1) yields

$$\frac{qv}{(m+\eta)} = V^*, S^* = \frac{((1-q)v+mV^*(t))}{(\eta+\beta I^*(t))}, E^* = \frac{(\beta S^*(t)I^*(t)+(1-\gamma)dT^*(t))}{(\psi+\eta)}, I^* = \frac{(\psi E^*(t)+\gamma dT^*(t))}{(\theta+\eta+\nabla)},$$

and $T^* = \frac{\theta I^*(t)}{(\eta+d+\phi)}$.

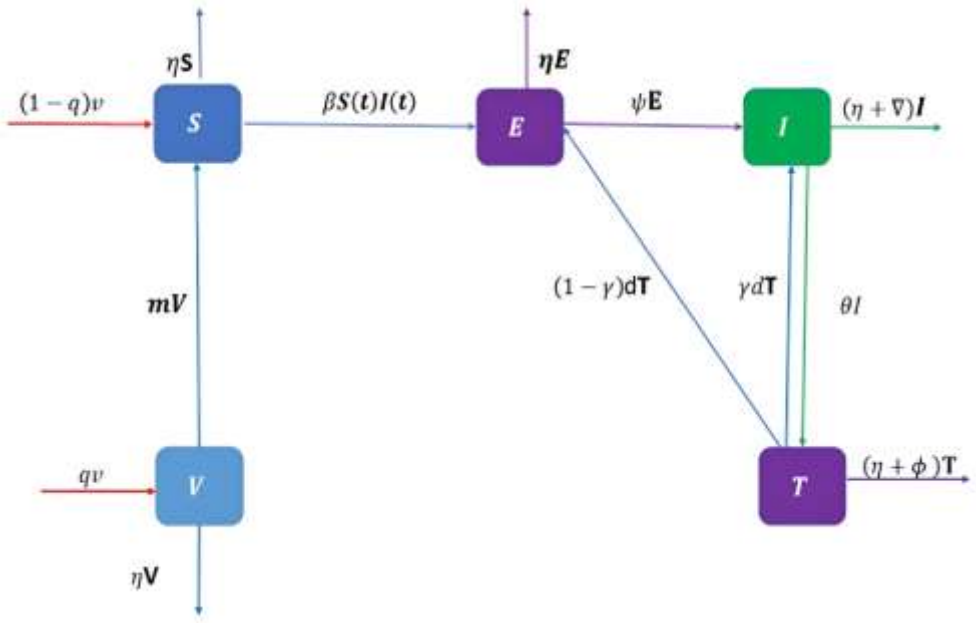

Figure 1. Flowchart of VSEIT model.

Variable	Description
$\boldsymbol{V(t)}$	The vaccinated population at time t.
$\boldsymbol{S(t)}$	The susceptible population which is able to be infected at any time t.
$\boldsymbol{E(t)}$	The exposed population, which is not yet infectious.
$\boldsymbol{I(t)}$	The infected population at time t.
$\boldsymbol{T(t)}$	The treated population at time t.
q	Vaccination rate
v	Recruitment rate
m	Rate of moving from V to S
η	Natural death rate
β	Transmission rate
ψ	Progression rate
γ	Treatment rate
θ	Treatment failure rate
∇	Disease death rate in I
d	Disease death rate in T

Table 1. Description of variable of the model (1).

3.2. Basic reproduction number ($\boldsymbol{R_0}$)

The reproduction number, an approximation provided by epidemiological research, can be used to estimate secondary infections, even if it is difficult to do so accurately (45). We make use of the matrices for translation and transmission, respectively, to calculate. The translation and transmission matrices are, respectively, determined.

$$F(x) = \begin{bmatrix} \beta S(t) I(t) \\ 0 \\ 0 \end{bmatrix}, \text{ and } V(x) = \begin{bmatrix} (\psi + \eta)E(t) - (1-\gamma)dT(t) \\ -\psi E(t) - \gamma dT(t) + (\theta + \eta + \nabla)I(t) \\ -\theta I(t) + (\eta + d + \phi)T(t) \end{bmatrix}.$$

As $R_0 = \rho(FV^{-1})$, therefore simple calculation employs

$$R_0 = \frac{\psi(\theta + \eta + \nabla \mathrm{q})\beta v p_3}{\eta(m+\eta)\big((p_1 p_2 p_3 - \psi\gamma d p_1 - (1-\gamma)\psi\gamma d)\big)}$$

4. Euler scheme

For model (1), Euler scheme can be created as shown below.

$$S_{n+1} = S_n + \Phi((1-q)v + mV_n(t) - \beta S_n(t) I_n(t) - \eta S_n(t))$$

Similarly,

$$V_{n+1} = V_n + \Phi(qv - (m+\eta)V_n(t))$$

and

$$E_{n+1} = C_n + \Phi(\beta S_{n+1}(t) I_n(t) - (\psi + \eta)E_{n+1}(t) + (1-\gamma)dT_n(t))$$

and

$$I_{n+1} = I_n + \Phi(\psi E_{n+1}(t) + \gamma dT_n(t) - (\theta + \eta + \nabla)\mathrm{I}_{n+1}(\mathrm{t}))$$
$$T_{n+1} = T_n + \Phi(\theta I_{n+1}(t) - (\eta + d + \phi)T_{n+1}(t))$$

4.1 The RK-4 Scheme

The RK-4 scheme is a common method that we use, especially when we don't have other instructions. To create the Rk-4scheme for system (1), we do this $S = K, V = L, E = M, I = N$ and $T = P$, then

Stage 1

$$K_1 = \Phi((1-q)v + mV_n(t) - \beta S_n(t) I_n(t) - \eta S_n(t))$$
$$L_1 = \Phi(qv - (m+\eta)V_n(t))$$
$$M_1 = \Phi(\beta S_n(t) I_n(t) - (\psi + \eta)E_n(t) + (1-\gamma)dT_n(t))$$
$$N_1 = \Phi(\psi E_n(t) + \gamma dT_n(t) - (\theta + \eta + \nabla)\mathrm{I}_n(\mathrm{t}))$$

$$P_1 = \Phi(\theta I_n(t) - (\eta + d + \phi)T_n(t))$$

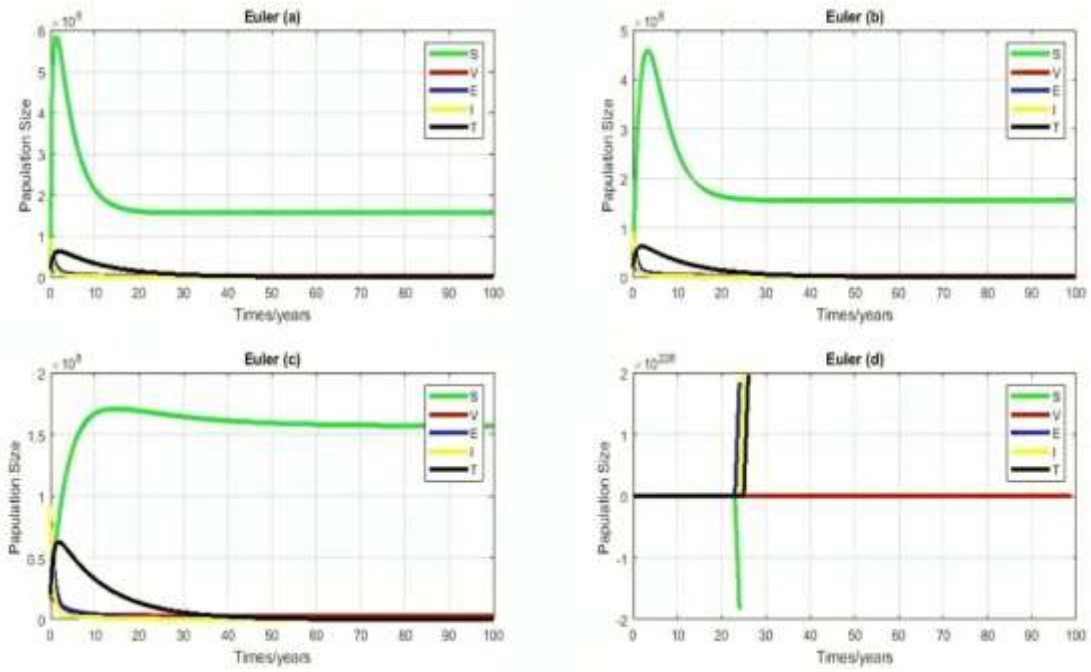

Figure 2. Numerical simulation for model by using Euler scheme (1)

In Figure 2, by using the Euler scheme with (a) 0.01 and (b). (a-c) Stable CFE point; other parameters remain fixed. Figure 2. (a, c) When used for calculations, Euler's TFE method produces accurate results. We saw in the picture Fig. 1.2 (d) that the TFE point becomes less steady (less powerful) as we take larger steps. Thus, we can conclude that when using really large steps, the Euler technique does not maintain a positive and stable situation.

Stage 3

$$K_3 = \Phi\left((1-q)v + m\left(V_n(t) + \frac{L_2}{2}\right) - \beta\left(S_n(t) + \frac{K_2}{2}\right)\left(I_n(t) + \frac{N_2}{2}\right) - \eta\left(S_n(t) + \frac{K_2}{2}\right)\right)$$

$$\mathrm{L}_3 = \Phi\left(qv - (m+\eta)\left(V_n(t) + \frac{L_2}{2}\right)\right)$$

$$\mathrm{M}_3 = \Phi\left(\beta\left(S_n(t) + \frac{K_2}{2}\right)\left(I_n(t) + \frac{L_2}{2}\right) - (\psi+\eta)\left(E_{n+1}(t) + \frac{M_2}{2}\right) + (1-\gamma)d\left(T_n(t) + \frac{P_2}{2}\right)\right.$$

$$N_3 = \Phi\left(\psi\left(E_n(t) + \frac{M_2}{2}\right) + \gamma d\left(T_n(t) + \frac{P_2}{2}\right) - (\theta + \eta + \nabla)\left(\mathrm{I}_n(\mathrm{t}) + \frac{N_2}{2}\right)\right)$$

$$P_3 = \Phi\left(\theta\left(I_n(t) + \frac{N_2}{2}\right) - (\eta + d + \phi)\left(T_n(t) + \frac{P_2}{2}\right)\right).$$

Stage 4

$$K_4 = \Phi\big((1-q)v + m(V_n(t)+L_3) - \beta(S_n(t)+K_3)(I_n(t)+N_3) - \eta(S_n(t)+K_3)\big)$$

$$\mathrm{L}_4 = \Phi\big(qv - (m+\eta)(V_n(t)+L_3)\big)$$

$$M_4 = \Phi(\beta(S_n(t)+K_3)(I_n(t)+L_3) - (\psi+\eta)(E_{n+1}(t)+M_3) + (1-\gamma)d(T_n(t)+P_4)$$

$$N_4 = \Phi\big(\psi(E_n(t)+M_3) + \gamma d(T_n(t)+P_3) - (\theta+\eta+\nabla)(\mathrm{I}_n(\mathrm{t})+N_3)\big)$$

$$P_4 = \Phi\big(\theta(I_n(t)+N_3) - (\eta+d+\phi)(T_n(t)+P_3)\big)$$

The final stage is

$$\Delta y_1 = \frac{1}{6}(K_1 + 2K_2 + 2K_3 + K_4)$$
$$\Delta y_2 = \frac{1}{6}(L_1 + 2L_2 + 2L_3 + L_4)$$
$$\Delta y_3 = \frac{1}{6}(M_1 + 2M_2 + 2M_3 + M_4)$$
$$\Delta y_4 = \frac{1}{6}(N_1 + 2N_2 + 2N_3 + N_4),$$
$$\Delta y_5 = \frac{1}{6}(P_1 + 2P_2 + 2P_3 + P_4),$$

Where $\Delta y_1, \Delta y_2, \Delta y_3$ and Δy_4 are the subjective of $k_\mathrm{i}, L_i, P_i \; and \; N_i$ where $i = \{1,2,3,4\}$.

Now,

$$y_{n+1} = y_n + \Delta y$$

We get

$$S_{n+1} = S_n + \frac{1}{6}(K_1 + 2K_2 + 2K_3 + K_4)$$
$$V_{n+1} = V_n + \frac{1}{6}(L_1 + 2L_2 + 2L_3 + L_4)$$
$$E_{n+1} = E_m + \frac{1}{6}(M_1 + 2M_2 + 2M_3 + M_4)$$
$$I_{n+1} = I_n + \frac{1}{6}(N_1 + 2N_2 + 2N_3 + N_4)$$
$$T_{n+1} = T_n + \frac{1}{6}(P_1 + 2P_2 + 2P_3 + P_4)$$

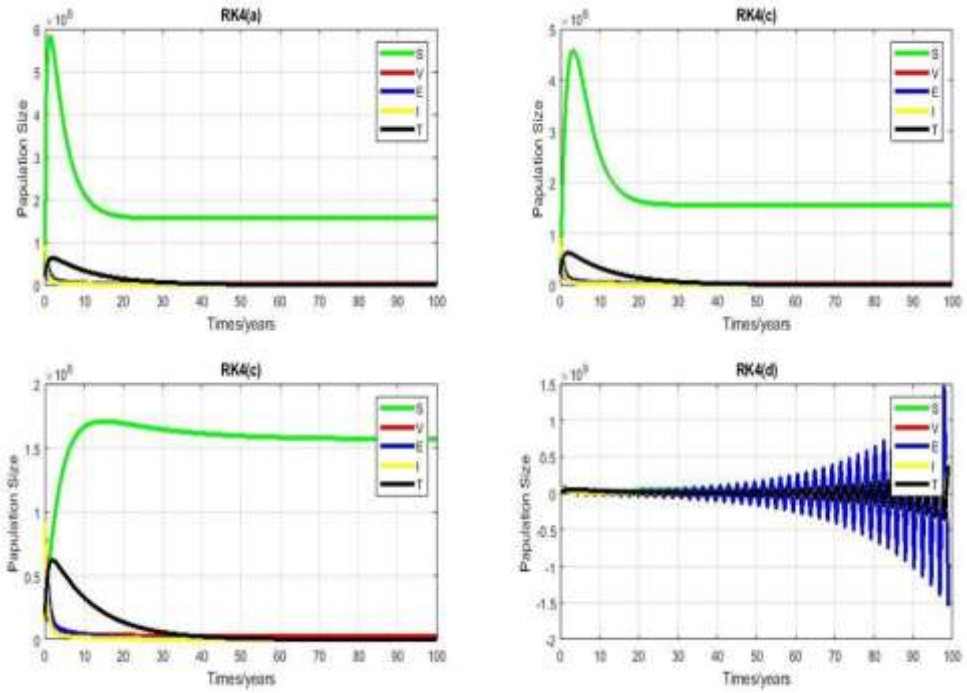

Figure 3. Numerical simulation for model (1) by using RK4- scheme

In Figure 3. with subfigures: (a) $h = 0.01$, (b) $h = 0.1, (c) h = 1, (d) h = 1.5$. (a-c) Stable TFE point with $v = 0.00498\ q = 0.977, m = 811085, \eta = 0.25$;other parameters remain fixed $\beta = 6.6752 * 10^{-11}, \psi = 0.0656, \gamma = 0.1095, \theta = 0.1325, \nabla = 1.0043, \phi = 0.002981, \mathcal{E} = 2.0136, d = 4.42327 * 10^{-6}, \psi = 0.0656, \gamma = 0.1095, d = 4.42327 * 10^{-6}$ When we utilize the RK-4 scheme for TFE, we observe favorable outcomes in Fig. 1.3 (a-c). But when we take large steps, it becomes less stable, as seen in Fig. 1.3 (d). Therefore, we draw the conclusion that the RK-4 strategy is ineffective for any step size.

4.2 Construction of NSFD scheme

The numerical estimates of $S(t), V(t), E(t), I(t)$ and $T(t)$ at $t = nh$ for model (1) are denoted as S_n, V_n, E_n, I_n, T_n, the nonnegative integer ' n ' represents the time for each step (46,47), and can be written based on model (1).

$$\frac{S_{n+1} - S_n}{\Phi} = (1-q)v + mV_{n+1}(t) - \beta S_{n+1}(t)I_n(t) - \eta S_{n+1}(t)$$

$$\frac{V_{n+1} - V_n}{\Phi} = qv - (m+\eta)V_{n+1}(t)$$

$$\frac{(E_{n+1} - E_n)}{\Phi} = \beta S_{n+1}(t)I_n(t) - (\psi + \eta)E_{n+1}(t) + (1-\gamma)dT_n(t)$$

$$\frac{I_{n+1} - I_n}{\Phi} = \psi E_{n+1}(t) + \gamma dT_n(t) - (\theta + \eta + \nabla)I_{n+1}(t) \qquad (2)$$

$$\frac{T_{n+1} - T_n}{\Phi} = \theta I_{n+1}(t) - (\eta + d + \phi)T_{n+1}(t$$

After rearrange the above terms

$$S_{n+1}(t) = \frac{\Phi(1-q)v + \Phi m V_{n+1}(t)}{(1+\Phi\beta I_n(t) + \eta\Phi)}$$
$$V_{n+1}(t) = \frac{\Phi q v + V_n}{(1+\Phi(m+\eta))}$$
$$E_{n+1}(t) = \frac{(\Phi\beta S_{n+1}(t) I_n(t) + \Phi(1-\gamma)dT_n(t) + E_n)}{(1+\Phi(\psi+\eta))}$$
$$\mathrm{I}_{n+1}(\mathrm{t}) = \frac{\Phi\psi E_{n+1}(t) + \Phi\gamma d T_n(t) + I_n}{\left(+\Phi(\theta+\eta+\nabla)\right)} \qquad (3)$$
$$T_{n+1}(t) = \frac{\Phi\theta I_{n+1}(t) + T_n}{(1+\Phi(\eta+d+\phi))}$$

4.3 Positivity and boundedness of NSFD scheme

Suppose the initial values of discrete scheme (3) are non-negative, i.e. $S_0 \geq 0, V_0 \geq 0, E_0 \geq 0, I_0 \geq 0, T_0 \geq 0$. As of the expectations, the expected values for these variables are also non-negative.: $S_n \geq 0, E_n \geq 0, I_n \geq 0, V_n \geq 0, T_n \geq 0$. Thus, solutions of NSFD scheme (3) indicate the positivity of scheme (3), i.e. $S_{n+1} \geq 0, E_{n+1} \geq 0, I_{n+1} \geq 0, V_{n+1} \geq 0, T_{n+1} \geq 0$. In order to discuss the boundedness of solutions of the NSFD system (4), we consider $P_n = S_n + +V_n + E_n + I_n + T_n$. Then

$$\frac{W_{n+1} - W_n}{\Phi} = v - \eta W_{n+1}$$

i.e.

$$(1+\psi\eta)W_{n+1} = \Phi v + W_n$$

Therefore, we get

$$W_{n+1} \leq \frac{\Phi v}{((1+\Phi\eta))} + \frac{W_n}{((1+\Phi\eta))} \Leftrightarrow \Phi v \sum_{k+1}^{m} \left(\frac{1}{((1+\Phi\eta)}\right)^k + W_0 \left(\frac{1}{(1+\Phi\eta)}\right)^m$$

If $0 < W(0) < \frac{v}{\eta}$, then by using Gronwall's inequality, we find

$$W_n \leq \frac{v}{\eta}\left(1 - \frac{1}{(1+\Phi\eta)^n}\right) + W_0 \left(\frac{1}{1+\Phi\eta}\right)^m = \frac{v}{\eta} + \left(W_0 - \frac{v}{\eta}\right)\left(\frac{1}{1+\Phi\eta}\right)^m \qquad (4)$$

Since $\left(\frac{1}{1+\Phi\eta}\right)^m < 1$, so we obtain $W_n \to \frac{\pi}{v}$ as $m \to \infty$. This shows that the solutions of the system (4) are bounded and the feasible region becomes

$$B = \left\{(V_n + S_n + E_n + I_n + T_n) : 0 \leq V_n + S_n + E_n + I_n + T_n \leq \frac{v}{\eta}\right\}. \qquad (5)$$

4.4 Local stability of equilibria

In order to demonstrate that the TFE point is locally asymptotically stable (LAS), we will apply the Schur-Cohn criterion (48,49) as definite in the following Lemma 1.

Lemma 1. The roots of $\mathrm{M}^2 - Q\mathrm{M} + L = 0$ guarantee $|\mathrm{M}_k| < 1$ for $k = 1,2$, $\Leftrightarrow$ the following requirements are satisfied.

1. $L < 1,$
2. $1 + Q + L > 0,$
3. $1 - Q + L > 0,$

where Q described trace and L mentioned determinant of the Jacobian matrix.

Theorem 1 if $\Phi > 0$, the TFE is LAS for NSFD model (4) when $R_0 < 1$.

Proof The Jacobian matrix can be expressed as the following using the data presented above

$$J(S,V,E,I,T) = \begin{bmatrix} \frac{\partial M_1}{\partial S} & \frac{\partial M_1}{\partial V} & \frac{\partial M_1}{\partial E} & \frac{\partial M_1}{\partial I} & \frac{\partial M_1}{\partial T} \\ \frac{\partial M_2}{\partial S} & \frac{\partial M_2}{\partial V} & \frac{\partial M_2}{\partial E} & \frac{\partial M_2}{\partial I} & \frac{\partial M_2}{\partial T} \\ \frac{\partial M_3}{\partial S} & \frac{\partial M_3}{\partial V} & \frac{\partial M_3}{\partial E} & \frac{\partial M_3}{\partial I} & \frac{\partial M_3}{\partial T} \\ \frac{\partial M_4}{\partial S} & \frac{\partial M_4}{\partial V} & \frac{\partial M_4}{\partial E} & \frac{\partial M_4}{\partial I} & \frac{\partial M_4}{\partial T} \\ \frac{\partial M_5}{\partial S} & \frac{\partial M_5}{\partial V} & \frac{\partial M_5}{\partial E} & \frac{\partial M_5}{\partial I} & \frac{\partial M_5}{\partial T} \end{bmatrix}, \qquad (6)$$

where M_1, M_2, M_3, M_4 and M_5 are provided in (5) a list of derivatives that can be found in (6) is as follows.

$$\frac{\partial M_1}{\partial S} = \frac{1}{(1 + \Phi\beta I_n(t) + \eta\Phi)'}, \frac{\partial M_1}{\partial V} = \frac{-\Phi m}{\left((1 + \Phi\beta I_n(t) + \eta\Phi)\right)^2}, \frac{\partial M_1}{\partial E} = 0, \frac{\partial M_1}{\partial I} = \frac{-1}{\left((1 + \Phi\beta I_n(t) + \eta\Phi)\right)^2}, \frac{\partial M_1}{\partial T} = 0, \frac{\partial M_2}{\partial S} = 0 \ \frac{\partial M_2}{\partial E} = 0 \ \frac{\partial M_2}{\partial I} = 0 \ \frac{\partial M_2}{\partial V} = \frac{1}{\left(1 + \Phi(m + \eta)\right)} \ \frac{\partial M_2}{\partial T} = 0, \frac{\partial M_3}{\partial S} = \frac{\Phi\beta I_n(t)}{\left(1 + \Phi(\psi + \eta)\right)} \ \frac{\partial M_3}{\partial E} = \frac{1}{\left(1 + \Phi(\psi + \eta)\right)} \ \frac{\partial M_3}{\partial V} = 0 \ \frac{\partial M_3}{\partial I} = \frac{\Phi\beta S_{n+1}(t) I_n(t)}{\left(1 + \Phi(\psi + \eta)\right)} \ \frac{\partial M_3}{\partial T} = \frac{\Phi(1 - \gamma)d}{\left(1 + \Phi(\psi + \eta)\right)}, \frac{\partial M_4}{\partial S} = 0, \frac{\partial M_4}{\partial E} = \frac{\Phi\psi}{\left(+\Phi(\theta + \eta + \nabla)\right)}, \frac{\partial M_4}{\partial V} = 0, \frac{\partial M_4}{\partial I} = \frac{1}{\left(+\Phi(\theta + \eta + \nabla)\right)}, \frac{\partial M_4}{\partial T} = \frac{\Phi\gamma d}{(+\Phi(\theta + \eta + \nabla))'} \frac{\partial M_5}{\partial S} = 0, \frac{\partial M_5}{\partial V} = 0, \frac{\partial M_5}{\partial E} = 0, \frac{\partial M_5}{\partial I} = \frac{\Phi\theta}{\left(1 + \Phi(\eta + d + \phi)\right)}, \frac{\partial M_5}{\partial T} = \frac{1}{(1 + \Phi(\eta + d + \phi))'}$$

Placing all the above derivatives in (6), we get

$$J = \begin{bmatrix} \frac{1}{(1+\Phi\beta I_n(t)+\eta\Phi)} & \frac{-\Phi m}{\left((1+\Phi\beta I_n(t)+\eta\Phi)\right)^2} & 0 & \frac{-1}{\left((1+\Phi\beta I_n(t)+\eta\Phi)\right)^2} & 0 \\ 0 & \frac{1}{(1+\Phi(m+\eta))} & 0 & 0 & 0 \\ \frac{\Phi\beta I_n(t)}{(1+\Phi(\psi+\eta))} & 0 & \frac{1}{(1+\Phi(\psi+\eta))} & 0 & 0 \\ 0 & 0 & \frac{\Phi\psi}{(+\Phi(\theta+\eta+\nabla))} & \frac{1}{(+\Phi(\theta+\eta+\nabla))} & \frac{\Phi\gamma d}{(+\Phi(\theta+\eta+\nabla))} \\ 0 & 0 & 0 & \frac{\Phi\theta}{(1+\Phi(\eta+\mathrm{d}+\phi))} & \frac{1}{(1+\Phi(\eta+d+\phi))} \end{bmatrix}. \quad (7)$$

At CFE point $E_0 = \left(\frac{qv}{(m+\eta)}, \frac{(1-q)v}{\eta}, 0,0,0\right)$, the matrix (7) becomes

$$J(E_0) = \begin{bmatrix} \frac{1}{(1+\eta\Phi)} & \frac{-\Phi m}{((1+\eta\Phi))^2} & 0 & \frac{-1}{((1+\eta\Phi))^2} & 0 \\ 0 & \frac{1}{(1+\Phi(m+\eta))} & 0 & 0 & 0 \\ 0 & 0 & \frac{1}{(1+\Phi(\psi+\eta))} & 0 & 0 \\ 0 & 0 & \frac{\Phi\psi}{(+\Phi(\theta+\eta+\nabla))} & \frac{1}{(+\Phi(\theta+\eta+\nabla))} & \frac{\Phi\gamma d}{(+\Phi(\theta+\eta+\nabla))} \\ 0 & 0 & 0 & \frac{\Phi\theta}{(1+\Phi(\eta+\mathrm{d}+\phi))} & \frac{1}{(1+\Phi(\eta+d+\phi))} \end{bmatrix}.$$

In demand to describe the eigenvalues, we adopt

$$|J(E_0) - I| = 0,$$

i.e.

$$\begin{bmatrix} \frac{1}{(1+\eta\Phi)}-\Lambda & \frac{-\Phi m}{((1+\eta\Phi))^2} & 0 & \frac{-1}{((1+\eta\Phi))^2} & 0 \\ 0 & \frac{1}{(1+\Phi(m+\eta))}-\Lambda & 0 & 0 & 0 \\ 0 & 0 & \frac{1}{(1+\Phi(\psi+\eta))}-\Lambda & 0 & 0 \\ 0 & 0 & \frac{\Phi\psi}{(+\Phi(\theta+\eta+\nabla))} & \frac{1}{(+\Phi(\theta+\eta+\nabla))}-\Lambda & \frac{\Phi\gamma d}{(+\Phi(\theta+\eta+\nabla))} \\ 0 & 0 & 0 & \frac{\Phi\theta}{(1+\Phi(\eta+d+\phi))} & \frac{1}{(1+\Phi(\eta+d+\phi))}-\Lambda \end{bmatrix} = 0 \quad (8)$$

Simple calculations, (8) yields

$$\left(\frac{1}{(1+\eta\Phi)}-\Lambda_1\right)\left(\frac{1}{(1+\Phi(m+\eta))}-\Lambda_2\right)\left(\frac{1}{(1+\Phi(\psi+\eta))}-\Lambda_3\right)\begin{vmatrix}\frac{1}{(+\Phi(\theta+\eta+\nabla))}-\Lambda & \frac{\Phi\gamma d}{(+\Phi(\theta+\eta+\nabla))}\\ \frac{\Phi\theta}{(1+\Phi(\eta+\mathrm{d}+\phi))} & \frac{1}{(1+\Phi(\eta+d+\phi))}-\Lambda\end{vmatrix}=0 \quad (9)$$

The equation (9) provides $\Lambda_1=\frac{1}{(1+\eta\Phi)}<1, \Lambda_2=\frac{1}{(1+\Phi(m+\eta))}<1$ and $\Lambda_3=\frac{1}{(1+\Phi(\psi+\eta))}<1$.

To find other eigenvalues, we take

$$\begin{vmatrix}\frac{1}{(+\Phi(\theta+\eta+\nabla))}-\Lambda & \frac{\Phi\gamma d}{(+\Phi(\theta+\eta+\nabla))}\\ \frac{\Phi\theta}{(1+\Phi(\eta+\mathrm{d}+\phi))} & \frac{1}{(1+\Phi(\eta+d+\phi))}-\Lambda\end{vmatrix}=0$$

i.e.

$$T^2-T\left(\frac{1}{(+\Phi(\theta+\eta+\nabla))}+\frac{1}{(1+\Phi(\eta+d+\phi))}\right)+\frac{\Phi\theta}{(1+\Phi(\eta+\mathrm{d}+\phi))}\frac{\Phi\gamma d}{(+\Phi(\theta+\eta+\nabla))}-\frac{1}{(1+\Phi(\eta+d+\phi))}\frac{1}{(+\Phi(\theta+\eta+\nabla))}=0. \quad (10)$$

1. $L<1$,
2. $1+Q+L>0$,
3. $1-Q+L>0$,

Comparing equation (10) with $T^2-QT+L=0$, we get $Q=\left(\frac{1}{(+\Phi(\theta+\eta+\nabla))}+\frac{1}{(1+\Phi(\eta+d+\phi))}\right)$ and $L=\frac{\Phi\theta}{(1+\Phi(\eta+\mathrm{d}+\phi))}\frac{\Phi\gamma d}{(+\Phi(\theta+\eta+\nabla))}-\frac{1}{(1+\Phi(\eta+d+\phi))}\frac{1}{(+\Phi(\theta+\eta+\nabla))}$. If $R_0<1$,

1. $L=\frac{\Phi\theta}{(1+\Phi(\eta+\mathrm{d}+\phi))}\frac{\Phi\gamma d}{(+\Phi(\theta+\eta+\nabla))}-\frac{1}{(1+\Phi(\eta+d+\phi))}\frac{1}{(+\Phi(\theta+\eta+\nabla))}<1.$
2. $1+D+E=1+\frac{1}{(+\Phi(\theta+\eta+\nabla))}+\frac{1}{(1+\Phi(\eta+d+\phi))}+\frac{\Phi\theta}{(1+\Phi(\eta+\mathrm{d}+\phi))}\frac{\Phi\gamma d}{(+\Phi(\theta+\eta+\nabla))}-\frac{1}{(1+\Phi(\eta+d+\phi))}\frac{1}{(+\Phi(\theta+\eta+\nabla))}>0$
3. $1-D+E=1-\frac{1}{(+\Phi(\theta+\eta+\nabla))}+\frac{1}{(1+\Phi(\eta+d+\phi))}+\frac{\Phi\theta}{(1+\Phi(\eta+\mathrm{d}+\phi))}\frac{\Phi\gamma d}{(+\Phi(\theta+\eta+\nabla))}-\frac{1}{(1+\Phi(\eta+d+\phi))}\frac{1}{(+\Phi(\theta+\eta+\nabla))}>0.$
4. In (2) when we put the numerical values of all positive parameter its gives us greater value of zero. So we can say that the point (2) is greater than zero.

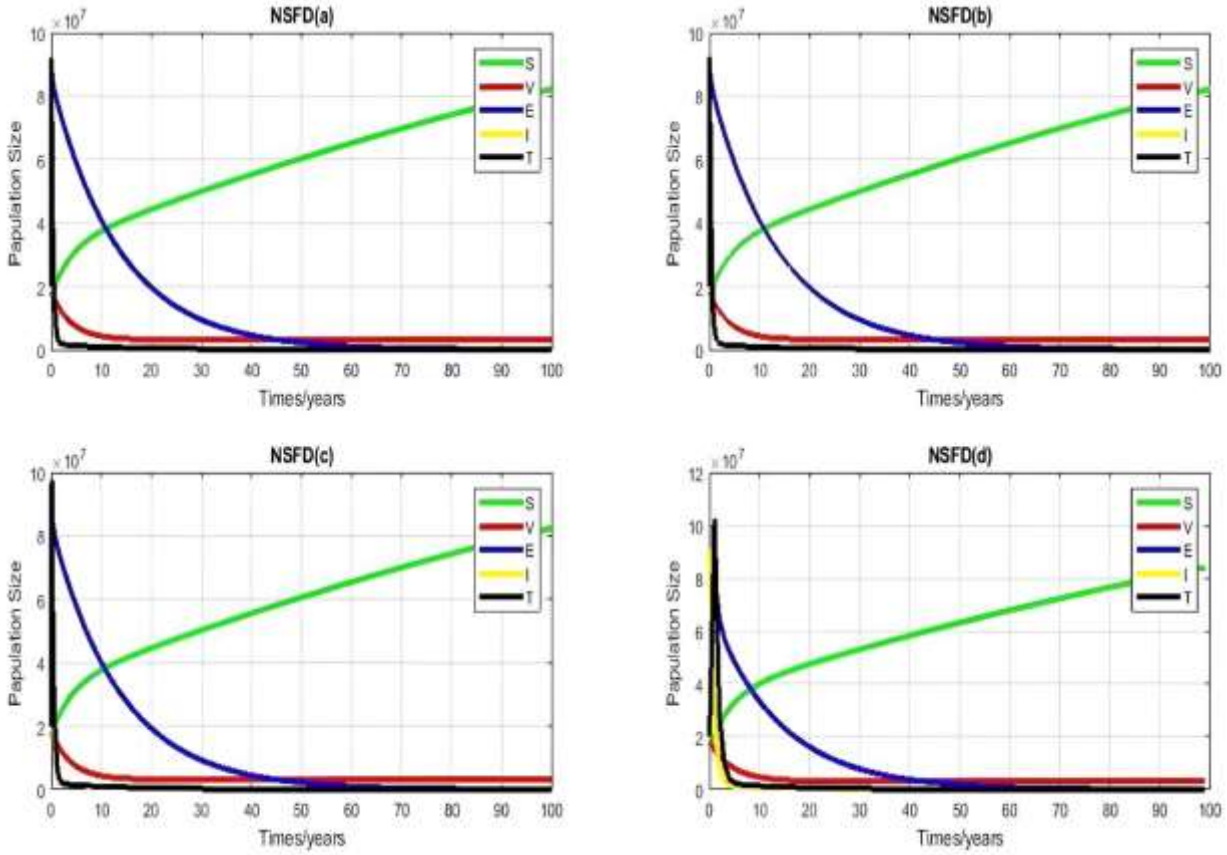

Figure 4. Numerical simulation for model (1) by using NSFD scheme.

In Figure 4, we can see the numerical simulation for model (1) by using the NSFD scheme with (a). (a-c) Stable CFE point with other parameters remaining fixed When we use the NSFD scheme for TFE, we see the results in Fig. 1.4 (a–d). However, if we take huge steps, it always shows stability for all steps. So, we can say that the NSFD scheme is in place for all steps that we take.

4.5 Global stability of equilibria

To find the global stability of TFE points for NSFD scheme (4), we describe the function $M(x) \geq 0$ such that $J(x) = y - \ln y - 1$ and, so $\ln y \leq y - 1$.

Theorem 3 For all $\psi > 0$, the CFE point is GAS for NSFD model (4) whenever $R_0 \leq 1$.

Proof Create a discrete Lyapunov function

$$U_n(S_n, V_n, E_n, I_n, T_n) = S^0 M\left(\frac{S_n}{S^0}\right) + \phi_1 V_n + \phi_2 E_n + \phi_3 I_n + \phi_4 T_n$$

where $\phi_k > 0$ for all $j = 1,2,3,4$. Hence, $X_n > 0$ for all $S_n > 0, E_n > 0, I_n > 0$, $H_n > 0$, and $R_n > 0$. In addition, $X_n = 0$, if and only if $S_n = S^0, V_n = V^0, E_n = E^0, I_n = I^0$, and $T_n =$

T^0. We take

i.e.

$$\Delta U_n = S^0 F\left(\frac{S_{n+1}}{S^0}\right) + \phi_1 V_{n+1} + \phi_2 E_{n+1} + \phi_3 I_{n+1} + \phi_4 T_{n+1} - \left(S^0 F\left(\frac{S_n}{S^0}\right) + \phi_1 V_n + \phi_3 E_n + I_n + \phi_3 T_n\right).$$

$$= S^0\left(\frac{S_{n+1}}{S^0} - \frac{S_n}{S^0} + \ln\frac{S_n}{S_{n+1}}\right) + \phi_1(V_{n+1} - V_n) + \phi_2(E_{n+1} - E_n) + \phi_3(I_{n+1} - I_n) + \phi_4(T_{n+1} - T_n). \quad (11)$$

Using the inequality $\ln y \le y - 1$, (11) becomes

$$\Delta U_n \le S_{n+1} - S_n + S^0\left(-1 + \frac{S_n}{S_{n+1}}\right) + \left(-1 + \frac{V_n}{V_{n+1}}\right)\varphi_1(V_{n+1} - V_n) + \left(-1 + \frac{E_n}{E_{n+1}}\right)\varphi_2(E_{n+1} - E_n) + \left(-1 + \frac{I_n}{I_{n+1}}\right)\varphi_3(I_{n+1} - I_n) + \left(-1 + \frac{T_n}{T_{n+1}}\right)\varphi_4(T_{n+1} - T_n).$$

$$= -\left(1 - \frac{S^0}{S_{n+1}}\right)(S_{n+1} - S_n) - \left(1 - \frac{V_n}{V_{n+1}}\right)\varphi_1(V_{n+1} - V_n) - \left(1 - \frac{E_n}{E_{n+1}}\right)\varphi_2(E_{n+1} - E_n) - \left(1 - \frac{I_n}{I_{n+1}}\right)\varphi_3(I_{n+1} - I_n) - \left(1 - \frac{T_n}{T_{n+1}}\right)\varphi_4(T_{n+1} - T_n). \quad (12)$$

By utilizing system (3), (12) can be written as

$$\Delta U_n \le -\left(\left(1 - \frac{S^0}{S_{n+1}}\right)\left((1-q)v + mV_{n+1}(t) - \beta S_{n+1}(t) I_n(t) - \eta S_{n+1}(t)\right) + \left(1 - \frac{V_n}{V_{n+1}}\right)\right.$$

$$\phi_1\left(qv - (m+\eta)V_{n+1}(t)\right) + \left(1 - \frac{E_n}{E_{n+1}}\right)\phi_2(\beta S_{n+1}(t) I_n(t) - (\psi + \eta)E_{n+1}(t) +$$

$$(1-\gamma)dT_n(t)) + \left(1 - \frac{I_n}{I_{n+1}}\right)\phi_3(\psi E_{n+1}(t) + \gamma d T_n(t) - (\theta + \eta + \nabla)\mathrm{I}_{n+1}(\mathrm{t})) + (1 -$$

$$\left.\frac{T_n}{T_{n+1}}\right)\phi_4(\theta I_{n+1}(t) - (\eta + d + \phi)T_{n+1}(t))\right). \quad (13)$$

Let φ_j for $j = 1,2,3,4$ be nominated so that

$$\phi_1(1-q)v + mV_{n+1}(t) - \beta S_{n+1}(t) I_n(t) - \eta S_{n+1}(t) = \phi_2(qv - (m+\eta)V_{n+1}(t)),$$
$$\phi_3(\beta S_{n+1}(t) I_n(t) - (\psi + \eta)E_{n+1}(t)) = \phi_4(\psi E_{n+1}(t) + \gamma d T_n(t) - (\theta + \eta + \nabla)\mathrm{I}_{n+1}(\mathrm{t})),$$
$$\left(\phi_3(\psi E_{n+1}(t) + \gamma d T_n(t) - (\theta + \eta + \nabla)\mathrm{I}_{n+1}(\mathrm{t}))\right) = \phi_4(\theta I_{n+1}(t) - (\eta + d + \phi)T_{n+1}(t)).$$

By putting the above values, from (13) we get

$$\Delta U_n \le -\left(\left(1 - \frac{S^0}{S_{n+1}}\right)((1-q)v + mV_{n+1}(t) - \beta S_{n+1}(t) I_n(t) - \eta S_{n+1}(t)) + \left(1 - \frac{V_n}{V_{n+1}}\right)\phi_1(qv - (m+\eta)V_{n+1}(t)) + \left(1 - \frac{E_n}{E_{n+1}}\right)\phi_2(\beta S_{n+1}(t) I_n(t) - (\psi + \eta)E_{n+1}(t)) + \left(1 - \frac{I_n}{I_{n+1}}\right)\phi_3(\psi E_{n+1}(t) + \gamma d T_n(t) - (\theta + \eta + \nabla)\mathrm{I}_{n+1}(\mathrm{t})) + \left(1 - \frac{T_n}{T_{n+1}}\right)\phi_4(\theta I_{n+1}(t) - (\eta + d + \phi)T_{n+1}(t))\right).$$

Simple calculations yields

$$\Delta U_n \leq -\left(\left(1-\frac{S^0}{S_{n+1}}\right)\left(v-\eta S_{n+1}(t)-\left(1-\frac{V_n}{V_{n+1}}\right)\phi_1(m+\eta)V_{n+1}(t)\right)+(1-\frac{E_n}{E_{n+1}}\right)\phi_2\beta S_{n+1}(t)I_n(t)+\phi_2\psi E_{n+1}+\phi_3\eta I_n+\left(1-\frac{I_n}{I_{n+1}}\right)\phi_3(\theta+\eta+\nabla)\mathrm{I}_{n+1}(\mathrm{t})+\phi_4 v E_n+\left(1-\frac{T_n}{T_{n+1}}\right)\phi_4(\eta+d+\phi)T_{n+1}(t)\Big).$$

$$\leq -\left((1-\frac{S_0}{S_{n+1}})\left(v--\eta S_{n+1}(t)-\left(1-\frac{V_n}{V_{n+1}}\right)\phi_1(m+\eta)V_{n+1}(t)+(1-\frac{E_n}{E_{n+1}}\right)\phi_2\beta S_{n+1}(t)I_n(t)-\left(1-\frac{I_n}{I_{n+1}}\right)\phi_4 v E_n+\left(1-\frac{T_n}{T_{n+1}}\right)\phi_4(\eta+d+\phi)T_{n+1}(t)\right)\right). \quad (14)$$

As $S^0=\frac{qv}{(m+\eta)}$ which implies $S^0q(m+\eta)=v$. By substituting π in (14), we obtain

$$\Delta X_n \leq -\left(1-\frac{S^0}{S_{n+1}}\right)\left(S^0q(m+\eta)-\eta S_{n+1}(t)-\left(1-\frac{V_n}{V_{n+1}}\right)\phi_1(m+\eta)V_{n+1}(t)+\left(1-\frac{E_n}{E_{n+1}}\right)\phi_2\beta S_{n+1}(t)I_n(t)-\left(1-\frac{I_n}{I_{n+1}}\right)\phi_4 v E_n+\left(1-\frac{T_n}{T_{n+1}}\right)\phi_4(\eta+d+\phi)T_{n+1}(t)\right).$$

$$=\frac{-q(m+\eta)}{S_{n+1}}\left((S_{n+1}-S^0)^2-\left(1-\frac{V_n}{V_{n+1}}\right)\phi_1(m+\eta)V_{n+1}(t)+(\eta+d+\phi)\,T_{n+1}(t)+\varphi_2\frac{\psi(\theta+\eta+\nabla\mathrm{q})\beta v p_3}{\eta(m+\eta)\big((p_1p_2p_3-\psi\gamma d p_1-(1-\gamma)\psi\gamma d)\big)}R_0\right).$$

Let $C_4=\frac{\psi(\theta+\eta+\nabla\mathrm{q})\beta v p_3}{\eta(m+\eta)\big((p_1p_2p_3-\psi\gamma d p_1-(1-\gamma)\psi\gamma d)\big)}$

$$=\frac{-q(m+\eta)}{S_{n+1}}\left((S_{n+1}-S^0)^2-\left(1-\frac{V_n}{V_{n+1}}\right)\phi_1(m+\eta)V_{n+1}(t)+(\eta+d+\phi)\,T_{n+1}(t)+\varphi_2 C_4R_0\right). \quad (15)$$

Hence, if $R_0\leq 1$ then from (19) employs $\Delta U_n\leq 0$ for all $n\geq 0$. Therefore, U_n is a nonincreasing sequence. So, here arises as a constant 0 such that $\lim_{n\to\infty}U_n=U$ which recommends $\lim_{n\to\infty}(U_{n+1}-U_n)=0$. From system (3) and $\lim_{n\to\infty}\Delta U_n=0$ we have $\lim_{n\to\infty}S_n=S^0$. For the case $R_0<1$, we have $\lim_{n\to\infty}S_{n+1}=S^0$ and $\lim_{n\to\infty}V_n=0, \lim_{n\to\infty}E_n=0$. From system (3), we attain $\lim_{n\to\infty}I_n=0, \lim_{n\to\infty}T_n=0$ and $\lim_{n\to\infty}T_n=0$. For the case $R_0=1$, we have $\lim_{n\to\infty}S_{n+1}=S^0$.Thus, from system (3), we obtain $\lim_{n\to\infty}T_n=0, \lim_{n\to\infty}I_n=0, \lim_{n\to\infty}E_n=0, \lim_{n\to\infty}T_n=0$ and $\lim_{n\to\infty}I_n=0$. Hence, E_0 is globally asymptotically stable.

5. Comparison

Here we show that NSFD is how much better than other methods (Euler, RK4) graphically represent as

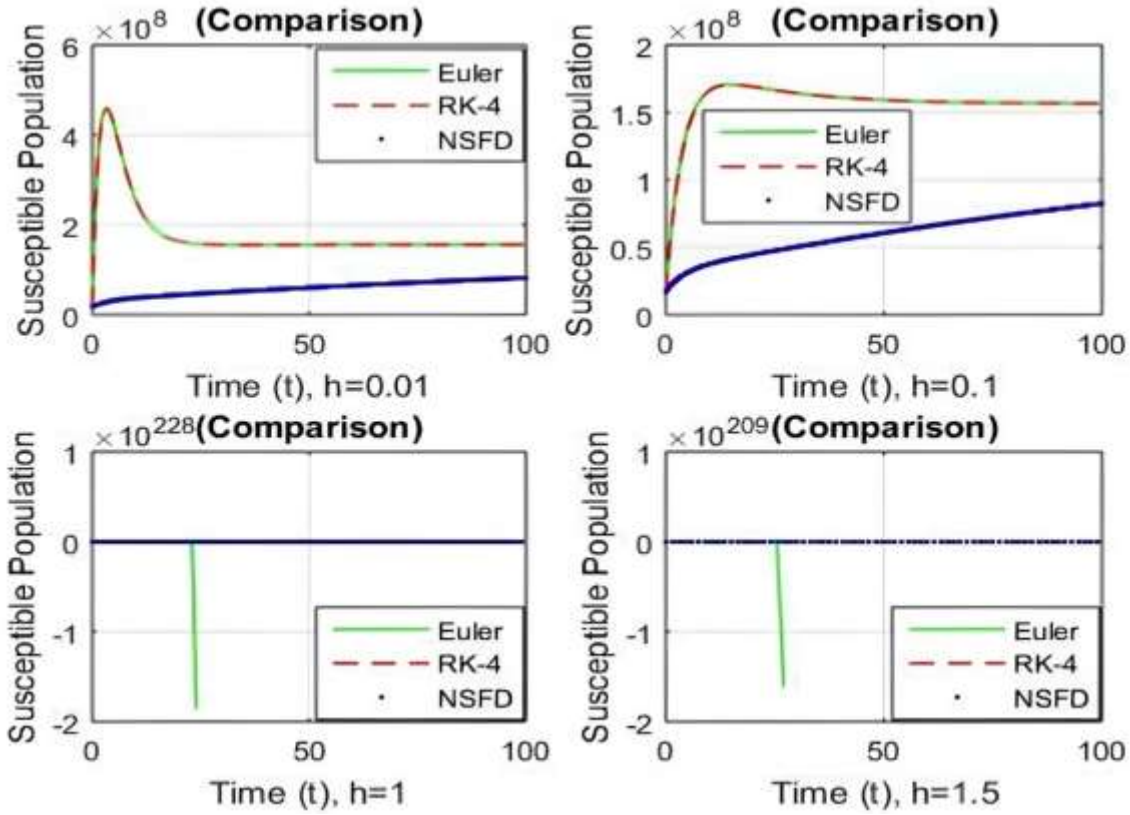

Figure 5. Numerical simulation for model (1) (a) $h = 0.01, (\ b)h = 0.1, (c)h = 1, (d)h = 1.5$. (a-c) Stable TFE point with $v = 0.00498, q = 0.977, m = 811085, \eta =$ 0.25 ;other parameters remain fixed $\beta = 6.6752 * 10^{-11}, \psi = 0.0656, \gamma = 0.1095, \theta = 0.1325, \nabla = 1.0043, \phi = 0.002981, \varepsilon = 2.0136, d = 4.42327 * 10^{-6}, \psi = 0.0656, \gamma = 0.1095, d = 4.42327 * 10^{-6}$

Conclusion

In this study, we used a mathematical model to analyze the spread of tuberculosis (TB) while considering both symptomatic and asymptomatic cases. To ensure the reliability and stability of key points in the model, we established a critical threshold value. We developed three algorithms—Euler, RK-4, and NSFD—for the continuous model. However, the accuracy of the Euler and RK-4 algorithms is affected by the step size, which can lead to unpredictable results. In contrast, the NSFD algorithm continuously converges regardless of the step size. We examined the stability of critical locations in the NSFD scheme by considering both local and global factors. Global stability was assessed by analyzing monotonic sequences. This approach helped to emphasize the similarities between discrete and continuous models, which could be beneficial for society and medicine. Finally, we presented our findings in Figures 2, 3, and 4, which could help predict the spread of TB.

Our research aims to delve into broader epidemic models in future investigations, enhancing our understanding of the dynamics of disease spread. To better understand disease transmission dynamics, we will combine sensitivity approaches with NSFD.

Data Availability

The data used to support the findings of this study are included within the article.

Conflicts of Interest

The author declare that he has no conflicts of interest.

References

1. World Health Organization. Global Tuberculosis Report. Geneva, Switzerland: World Health Organization,, 2023. Available from: https://extranet.who.int/tme/generateCSV.asp?ds=notifications (accessed on 1 January 2023).

2. Narain R, Nair SS, Naganna K, Chandrasekhar P, RaoGR, and GR, and Lal P. Problems in defining a "case" of pulmonary tuberculosis in prevalence surveys. Bull World Health Organ. 1968;39(5):701.

3. Schwartz,Schwartz, SH. An overview of the Schwartz theory of basic values. Online readings in Psychology andCulture, 2012, 2(1):11. Culture, 2012, 2(1):11.

4. Hamer WH. The Milroy lectures on epidemic diseases in England: The evidence of variability and of persistency of type; delivered before the RoyalRoyal CollegeCollege of PhysiciansPhysicians of London, March 1st, 6th, and 8th, 1906. Bedford Press,, 1906.

5. Martini E. Berechnungen und Beobachtungen fur EpidemiologieEpidemiologie und Bekämpfung der Malaria auf GrundGrund von Balkanerfahrungen. W. Genet. Lota AJ. Elements of PhysicalPhysical Biology Biology Williams & Wilkins,, 1921, 1925.

6. Frimodt-Møller J. A community-wide tuberculosis survey in a South Indian rural population, 1950–551950–55. Bull World Health Organ. 1960;22(12):61.

7. Kermack WO, McKendrick AG. A contribution to the mathematical theory of epidemics. Proc R Soc Lond A. 1927;115(772):700–7211927;115(772):700–721.

8. Ullah S.S., Khan MA, FarooqM., and M., and Gul T. Modeling and analysis of tuberculosis (TB) in Khyber Pakhtunkhwa, Pakistan. Math Comput Simul. 2019;165:181–1992019;165:181–199.

9. Ucakan Y, GulenS, and S, and Koklu K. Analyzing tuberculosis in Turkey through SIR, SEIR,SEIR, and BSEIR mathematical models. Math Comput Model Dyn Syst. 2021;27(1):179–2022021;27(1):179–202.

10. Egonmwan AO, Okuonghae D. Mathematical analysis of a tuberculosis model withan imperfect an imperfect vaccine. Int J Biomath. 2019;12(07):1950073.

11. Revelle CS, LynnWR, and WR, and Feldmann F. Mathematical models for the economic allocation of tuberculosis control activities in developing nations. Am Rev Respir Dis. 1967;96(5):893-909.

12. Hedrich AW. Monthly estimates of the child population "susceptible" to measles, 1900–19311900–1931, Baltimore, MD. Am J Epidemiol. 1933;17(3):613-636.

13. Bernoulli D.D., Chappelle D. Essay dune nouvelle analyses de la mortality cause par la petite virile et des avantagesavantages de inoculation pourpour la prévenir. 2023.

14. Muench H.,H., Catalytic ModelsModels in Epidemiology,Epidemiology, Harvard University Press,, 1959.

15. Raza A.A., Rafiq M.M., Awrejcewicz J.J., AhmedN., and N., and Mohsin M. Dynamical analysis of coronavirus disease with crowding effect and vaccination: a study of the third strain. Nonlinear Dyn. 2021;107(4):3963–39822021;107(4):3963–3982.

16. Avilov KK, Romanyukha AA. Mathematical Models of Tuberculosis Extension and Control of It. It. Math Biol Bioinform. 2007;2(2):188–318. 2007;2(2):188–318. Mathematical Biology, 2(2).

17. Hamer WH. The Milroy lectures on epidemic diseases in England: The evidence of variability and of persistency of type; delivered before the RoyalRoyal CollegeCollege of PhysiciansPhysicians of London, March 1st, 6th, and 8th, 1906. Bedford Press,, 1906.

18. Martini E. Berechnungen und Beobachtungen fur EpidemiologieEpidemiologie und Bekämpfung der Malaria auf GrundGrund von Balkanerfahrungen. W. Genet. Lota AJ. Elements of PhysicalPhysical Biology Biology Williams & Wilkins,, 1921, 1925.

19. Frimodt-Møller J. A community-wide tuberculosis survey in a South Indian rural population, 1950–55. 1950–55. Bull World Health Organ. 1960;22(1-2):61.

20. Kermack WO, McKendrick AG. A contribution to the mathematical theory of epidemics. Proc R Soc Lond A. 1927;115(772):700–721.

21. Andersen P, Doherty TM. The success and failure of BCG: implications for a novel tuberculosis vaccine. Nat Rev Microbiol. 2005;3(8):656–662.

22. Ucakan Y, Gulen S, and Koklu K. Analyzing tuberculosis in Turkey through SIR, SEIR, and BSEIR mathematical models. Math Comput Model Dyn Syst. 2021;27(1):179–202.

23. Egonmwan AO, Okuonghae D. Mathematical analysis of a tuberculosis model with an imperfect vaccine. Int J Biomath. 2019;12(07):1950073.

24. Li MY, Muldowney JS. Global stability for the SEIR model in epidemiology. Math Biosci. 1995;125(2):155–164.

25. Newton EA, Reiter P. A model of the transmission of dengue fever with an evaluation of the impact of ultra-low volume (ULV) insecticide applications on dengue epidemics. Am J Trop Med Hyg. 1992;47(6):709–720.

26. Singh JP, Kumar S, Baleanu D, and Nisar KS. Monkeypox Viral Transmission Dynamics and Fractional-Order Modeling with Vaccination Intervention. Fractals. 2023 Sep 23:2340096.

27. Singh JP, Abdeljawad T, Baleanu D, and Kumar S. Transmission dynamics of a novel fractional model for the Marburg virus and recommended actions. The European Physical Journal Special Topics. 2023 Nov;232(14):2645–55.

28. Wang Y, Cao J. Global stability of general cholera models with nonlinear incidence and removal rates. J Franklin Inst. 2015;352(6):2464-2485.

29. Chennaf B, Abdelouahab MS, and Lozi R. Analysis of the Dynamics of Tuberculosis in Algeria Using a Compartmental VSEIT Model with Evaluation of the Vaccination and Treatment Effects. Computation. 2023;11(7):146.

30. Diekmann O, Heesterbeek JAP, and Metz JA. On the definition and computation of

the basic reproduction ratio R0 in models for infectious diseases in heterogeneous populations. J Math Biol. 1990;28:365–382.

31. Mickens, RE. Nonstandard finite difference models of differential equations. World Scientific; 1994.

32. Mickens RE. Dynamic consistency: a fundamental principle for constructing nonstandard finite difference schemes for differential equations. J Difference Equ Appl. 2005;11(7):645–653.

33. Vieira A. and Kailath T. on another approach to the Schur-Cohn criterion. IEEE Trans Circuits Syst. 1977;24(4):218–220.